The Conditional Handover Parameter Optimization for 5G Networks

Original Scientific Paper

Zolzaya Kherlenchimeg

National University of Mongolia, School of Information Technology and Electronics Oyutnii gudamj 14/3, Ulaanbaatar, Mongolia zolzayakhh@num.edu.mn

Battulga Davaasambuu*

National University of Mongolia, School of Information Technology and Electronics Oyutnii gudamj 14/3, Ulaanbaatar, Mongolia battulgad@num.edu.mn

Telmuun Tumnee

National University of Mongolia, School of Information Technology and Electronics Oyutnii gudamj 14/3, Ulaanbaatar, Mongolia telmuun@num.edu.mn

*Corresponding author

Nanzadragchaa Dambasuren

National University of Mongolia, School of Information Technology and Electronics Oyutnii gudamj 14/3, Ulaanbaatar, Mongolia nanzadragchaa@num.edu.mn

Di Zhang

School of Intelligent Systems Engineering, Sun Yat-sen University, Shenzhen 518107, China zhangd263@mail.sysu.edu.cn

Ugtakhbayar Naidansuren

National University of Mongolia, School of Information Technology and Electronics Oyutnii gudamj 14/3, Ulaanbaatar, Mongolia uqtakhbayar@num.edu.mn

Abstract – Conditional Handover (CHO) is a state-of-the-art handover technique designed for 5G and beyond networks. It decouples the preparation and execution phases of the traditional handover process and aims to reduce wrong cell selection by utilizing a predefined list of target cells. Despite its advantages, the limitations of static parameter configuration compromise CHO performance. This paper proposes a self-optimization mechanism for CHO parameters in 5G networks. Our proposed mechanism is an automated method for estimating and optimizing CHO parameters, dynamically adjusting key parameters to fine-tune the conditions that trigger the execution phase of the handover process. In addition, we introduce a second handover trigger referred to as the cell outage condition. We compared the performance of our proposed mechanism with the baseline CHO, velocity-based, and cell-outage based mechanisms, using Ping-Pong Handovers (PPHO) and Radio Link Failures (RLF). The simulation results demonstrate reduction of up to 7% in RLF, a 0.15% decrease in handover errors, and an improvement of approximately 10% in handover performance at velocities of up to 200 km/h in high-mobility scenarios.

Keywords: mobile networks, conditional handover, handover performance, optimization

Received: May 2, 2025; Received in revised form: July 2, 2025; Accepted: July 2, 2025

1. INTRODUCTION

Fifth generation (5G) mobile technology has significantly impacted daily life by enabling new features such as the Internet of Things (IoT), massive machine-type communications (mMTC), Ultra-Reliable Low-Latency Communications (URLLC) and vehicular networks (V2X) [1]. Next generations of mobile networks, including 5G-Advanced and Beyond 5G (B5G), aim to support even higher data rates, near-zero latency, and ubiquitous connectivity [1, 2]. In addition, B5G integrates artificial intelligence for network optimization, employs terahertz (THz) communication bands to en-

able extreme bandwidth, holographic and tactile Internet applications, and holistic network coverage integrating terrestrial, aerial, and satellite segments [1,2].

5G networks also use dual-connectivity and multiconnectivity techniques to improve connectivity and overall performance. Using mm-wave frequencies enables denser cellular networks to meet higher data throughput requirements. However, these challenges include moving mobile users and requiring frequent handovers between microcells. Handover processes in mobility management ensure that users maintain uninterrupted connectivity during cell transitions. The 5G literature has introduced three primary handover techniques to minimize interruption time and reduce handover failures. The first two techniques have been developed to address dual-connection and multi-connection scenarios. In 5G and beyond networks, the slicing technique is an important virtualization [3]. It is also necessary to define the procedures for handover between slices.

The third technique, CHO, is a cutting-edge mechanism specifically designed for 5G homogeneous networks [4,5]. The CHO is developed to decouple the preparation and execution phases of the traditional handover process and aims to reduce wrong cell selection by utilizing a predefined list of target cells [6]. Also, it was initially introduced to enhance service quality and reliability for users with single connectivity within homogeneous networks. In the paper [7], the authors have dedicated their efforts to refining the CHO process, particularly to minimizing wrong target-cell selections during the preparation phase. If the wrong target cell is selected, the handover process fails in the execution phase, and the user equipment (UE) reconnects to the serving cell. The UE then initiates a new handover procedure, resulting in temporary unavailability of the user's data path and an extended service interruption time.

The adoption of CHO in 5G networks offers notable benefits, but also increases control messages, which strains network management [8]. Also, deploying and configuring multiple conditions with static parameters in CHO may adversely effect overall network performance [9]. To address the challenge of CHO, we propose a parameter self-optimization mechanism for CHO in 5G networks. Our Autotuning-based Parameters for Conditional Handover (APCHO) mechanism estimates and optimizes the trigger parameters of CHO. Our main contributions are as follows:

- We formulate an auto-tuning mechanism for the offset parameter in CHO's execution condition to reduce handover errors. Our mechanism estimates the offset parameter based on the UE's velocity, which serves as the main handover trigger.
- We propose an efficient cell outage condition that is related to cell size. Our mechanism uses this condition as an additional trigger for the handover procedure. This mechanism helps to manage late and early handovers and improve the efficiency of handover procedures in 5G HetNets.
- Furthermore, our APCHO mechanism uses an approach based on mobility management performance data to dynamically adjust the weight of parameters to mitigate the effect of handover errors.

The paper is organized as follows. Section I provide an overview of the topic, while Section II introduces the background and related works. In Section III details the proposed mechanism. Section IV presents the simulation setup and results. Finally, Section V concludes the paper with final remarks.

2. BACKGROUNDS OF CONDITIONAL HANDOVER

This section provides an overview of CHO and Handover Performance Indicator (HPI), and related works.

2.1. CONDITIONAL HANDOVER

Mobile networks use a handover mechanism comprising three phases: preparation, execution, and completion. The cell to which the UE is currently connected cell, called the serving cell, begins the preparation phase with a measurement command. In response, the UE returns the measurement results to the serving cell. Based on the measurement results, the serving cell identifies a suitable cell called the target cell for the user's transition and sets the trigger for the execution phase. In the completion phase, the serving cell releases the radio resources and other configurations based on the handover completion message received from the target cell.

The CHO involves three conditions: adding cells to the target cell list, removing cells from the target cell list and initiating the execution phase, as shown in Fig. 1. For example, if the add condition is met (case number 1 in blue on Fig. 1), the serving cell adds a target cell 1 to the target cell list. Additionally, the UE measures the signal strength of all cells in the target cell list by activating a measurement command until the target cell's signal strength meets the other two conditions, and the serving cell sends a request to reserve and configure radio resources of target cells for the UE [8]. On the other hand, if the remove condition is met (case number 3 in blue on Fig. 1), target cell 1 is removed from the target cell list. Then, the radio resources of target cell 1 are released. These three conditions are part of the preparation phase.

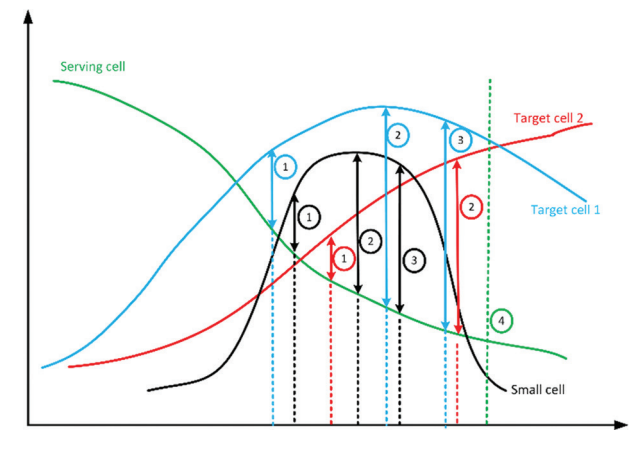


Fig. 1. CHO procedures

Figure 1 also shows the CHO procedures for target cell 1, microcell and cell outage threshold of the serving cell. If all parameters are statically configured and the serving cell's (case number 4 in green on Fig. 1) cell outage threshold is not met, the UE begins the execution phase for handover to a microcell.

The UE is transferred to a smaller cell, and a new CHO procedure starts after a certain time.

Once the execution condition (case number 2 in blue on Figure 1) is met, the UE begins transitioning to the designated target cell at the beginning of the execution phase. Once completing the execution phase, the handover process moves to the completion phase. During this stage, the newly connected cell becomes the new serving cell, and releases the radio resources associated with the previous serving cell as well as those from the target cell list. The three conditions of CHO are introduced below [10].

Equation 1 shows the add condition of CHO.

$$RSRP_{target} \ge RSRP_{serving} + o_{add}$$
 (1)

where RSRP_{target} and $\mathit{RSRP}_{serving}$ are the target and the serving cell's Reference Signal Received Power (RSRP), and o_{add} is the offset for all candidate cells listed in the measurement report.

 The remove condition of CHO is introduced in Equation 2.

$$RSRP_{target} \ge RSRP_{serving} - o_{remove}$$
 (2)

where $RSRP_{target}$ and $RSRP_{serving}$ are the RSRP of the target and the serving cell, and o_{remove} is the offset for all cells in the target cell list.

The UE initiates the execution phase by establishing a new connection with a target cell that satisfies Equation 3.

$$RSRP_{target} \ge RSRP_{serving} + o_{exec}$$
 (3)

where $RSRP_{target}$ and $RSRP_{serving}$ are the RSRP of the target and the serving cell, and $o_{\it exec}$ is the offset for all cells in the target cell list.

In summary, CHO introduces the following changes during the preparation and execution phases: a) separation of handover phases to operate independently, enhancing efficiency and reliability; b) creation of a target cell list based on the measurement results for cell selection; c) establishment of clear criteria for adding, removing, and executing handover conditions; and d) pre-configuration of radio resources for all target cells, minimizing transition delays. However, the implementation of CHO presents several constraints:

- A substantial increase in the exchange of control messages.
- Heightened intricacy in prioritizing cells within the target cell list.
- A well-refined algorithm is needed to select the appropriate target cell for execution initiation.
- The need to fine-tune parameter values for conditions.
- The need to optimize execution criteria to initiate handover at the most reasonable time.

2.2. HANDOVER PERFORMANCE INDICATORS

In the context of handover parameter optimization, researchers have introduced metrics to evaluate handover performance. In Saad et al. [11], indicators such as handover probability, ping-pong handover probability, and outage probability are introduced as measures of handover performance. Additionally, the authors analyzed the impact of these handover indicators and conducted a performance analysis of the proposed optimization mechanism in a simulation environment.

HPI is defined as a metric for monitoring the performance of handover procedures for each cell pair. The calculation of HPI involves summing three indicators: Handover Failure (HOF), Handover Ping-Pong (HPP), and Radio Link Failure (RLF). We define HPI as the sum of these indicators.

$$HPI = \omega_{HPP} * HPP + \omega_{RLF} * RLF + \omega_{HOF} * HOF$$
 (4)

where $\omega_{HPP'}$ $\omega_{RLF'}$ and ω_{HOF} are the weights for each indicator of handover performance.

These include:

HPP refers to a ping-pong handover, where the UE begins a new handover procedure to the serving cell after a successful handover to the target cell.
HPP is the ratio of ping-pong handovers to total handovers attempted handovers (HO).

$$HPP = \frac{number\ of\ ping-pong}{total\ HO} \tag{5}$$

where number of *ping-pong* is the number of ping-pong handovers, and *total HO* is all attempted handovers.

RLF can occur when the UE moves out of the coverage area of the serving cell before or during the handover process. RLF is defined as the ratio of the number of radio link failures (RLFs) to the total number of attempted HO.

$$RLF = \frac{number\ of\ RLF}{total\ HO} \tag{6}$$

where the *number of RLF* is the number of RLFs, and the total HO is all attempted handovers. *RLF* indicates the frequency of RLF.

 HOF is the ratio of the number of handover failures to the total number of attempted handovers. Additionally, HOF also includes wrong cell selection.

$$HOF = \frac{number\ of\ handover\ failures}{total\ HO} \tag{7}$$

where the number of *handover failures* refers to all handover failure events, and the total *number of* attempted handovers.

2.3. RELATED WORKS

Many studies have focused on CHO and its improvements. The fast conditional handover (FCHO), introduced in [12, 13], enhances the handover process by retaining the target cell list after completion of a

conditional handover (CHO). This allows subsequent handovers to be performed independently, without repeating the full preparation steps, such as configuration and measurements. As a result, FCHO significantly reduces both mobility failures and signaling overhead, as demonstrated in experimental evaluations. In [14], the authors first analyzed real-world data collected from a mobile network to study its configuration and performance. They then improved Iqbal et al.'s FCHO by adapting target cell selection criteria tailored for public transit systems. While their approach effectively reduces signaling overhead in public transportation scenarios, it has limitations, including being specifically designed for a particular use case and not considering velocity in the mobility model. In other words, it focuses on demonstrating parameter selection for specific environments.

In [15], the authors investigated the reallocation of resources during the CHO preparation phase. During target cell evaluation, they utilized beam-specific measurement reports to update Contention Free Random Access (CFRA) resources. The advantage of this approach was demonstrated through experimental results showing reductions in average handover delay and handover failures. However, the results indicated that relying solely on resource allocation was insufficient to significantly improve delay and failure rates.

In [16], the authors proposed an Al-based approach to address measurement report challenges in nonterrestrial networks, where the distance between the user and the base station is significant. Their method involves predicting the handover execution point in the two-step process based on the outcome of the one-step phase. The key experimental finding was that unnecessary handovers and ping-pong handovers occurred more frequently than RLF and HOF, highlighting a significant limitation in the handover decision process. Another notable work on Al-based signal overhead reduction is presented in [17]. The authors introduce an Al-assisted conditional handover using a classifier that performs CHO preparations and manages measurement reports to reduce unnecessary signaling. In this approach, the measurement reports are classified as necessary or unnecessary based on the signal strength received by the user from the base station. According to the simulation results, this method reduced signaling overhead by 53%, and other indicators such as RLF also showed a significant decrease.

In [18], the authors presented a method for adjusting handover hysteresis and time-to-trigger (TTT) based on different UE velocities and RSRP values. The proposed approach demonstrated a reduced ratio of handover failures to total handover through simulation results. Moreover, the mechanism significantly lowered the average number of ping-pong handovers and handover failures compared to other schemes. While the study is similar to ours in showing the relationship between velocity and handover performance, it differs in that it does not take performance-based actions.

Deb et al. [19] presents an analytical evaluation of CHO performance, proposing a Markov model with offsets, time-to-preparation, and time-to-execution. Through experiments and analysis, Deb [19,20] demonstrates that channel fading plays a crucial role in reducing handover failure and latency. The impact of CHO parameters on user velocity is analyzed. Although multiple static configurations of the parameters were tested in the experiments, the results indicate that static tuning alone is insufficient.

Among many Al-based approaches, we focused on those most similar to our work in terms of optimization objectives, performance indicators, and simulation-based evaluation. In [21], Kwon et al. proposed a deep learning-based mechanism to optimize handover in 5G networks by dynamically adjusting the hysteresis value. Their method considered key performance indicators, including handover failures, ping-pong handovers, throughput, and latency. The experimental results demonstrated high throughput and low latency, particularly in high-mobility scenarios.

In Lee et al. [22], a prediction-based deep-learning approach for 5G mmWave networks is discussed. The proposed approach uses deep learning to predict the next base station, making it a compelling method that learns from previously executed handovers to support decision-making and prediction. The researchers' experiments showed that the proposed method achieved an accuracy of 98.8%. By reducing the wrong cell selection, the overall handover performance was improved. In [23], tests were conducted on a 5G emulator with user speeds ranging from 20 to 130 km/h. The proposed adaptive mechanism makes optimal handover decisions based on Received Signal Strength Indicator (RSSI), user direction, and velocity. Experimental results showed that at higher speeds, RSSI decreased, negatively affecting service quality. For example, handover latency was 8 ms at a speed of 80 km/h, and increased to 12 ms at 130 km/h.

Yin et al. propose an approach that combines the advantages of traditional handover and conditional handover (CHO) [24]. In the cell selection phase, the target cell list for CHO is defined with limitations—the selection is based not only on the strongest signal but also on the user's historical handover data. The execution phase is triggered by using the traditional handover execution condition (Event A4). Experimental results showed that, compared to CHO alone, the proposed method reduced total handover failures. However, it also led to an increase in handover attempts, which is a drawback. In [25], the researchers proposed a Q-learning-based reinforcement learning approach for handover decision optimization. Overall, this method aims to improve QoS by reducing handover failures and ping-pong handovers while enhancing overall performance. However, to achieve optimal handover decisions, the approach requires repeated actions over time, which leads to increased processing delays. Additionally, the computational complexity of the method is relatively high.

A reinforcement learning-based adaptive handover approach with optimized decision-making for 5G mmWave bands is presented in [26]. The proposed method predicts the reference signal received power (RSRP) of the target gNB, selects the best target cell from a neighboring cell list, and dynamically determines the handover trigger and hysteresis values. The study analyzes handover success rate, delay, latency, and user throughput using a high-mobility model with speeds up to 200 km/h in an urban test environment. While the handover success rate improved, and handover delay decreased, the approach faces challenges related to computational resource demands and complexity when applied in HetNet environments.

Sattar et al [27] presents a novel rectangular microstrip patch antenna designed for 28 GHz using FR4 substrate, where three feeding techniques are analyzed, showing that proximity coupling significantly enhances gain (from 5.50 dB to 6.83 dB) and bandwidth (from 0.6 GHz to 3.60 GHz), making the antenna highly suitable for 5G applications. [2,28] propose a self-optimization approach for handover hysteresis and timeto-trigger (TTT). This method incorporates 5G network KPIs such as handover probability, handover failures, ping-pong handovers, and radio link failures (RLF) into its calculations. Experiments were conducted at speeds up to 120 km/h, and the results compared three mechanisms. Among them, the velocity-based approach achieved a handover attempt rate similar to the others, while significantly reducing ping-pong handovers and handover failures.

3. AUTOTUNING-BASED PARAMETERS FOR CONDITIONAL HANDOVER

The seamless mobility between cells through efficient handover processes is essential for maintaining high-quality service in cellular networks. Service interruptions or errors during handovers can significantly degrade network performance, resulting in increased latency, reduced data throughput, and connection interruptions. We present an APCHO mechanism that automatically adjusts the parameter values to address these challenges. APCHO automatically changes crucial parameters, such as offsets and the cell outage threshold, based on different network environments and the user's velocity. A distinguishing feature of APCHO is its dual-trigger decision framework. One of the key advantages is that APCHO incorporates the threshold of cell outage as an additional condition, where serves as a second trigger for the handover execution phase.

3.1. AUTO-TUNING PARAMETERS

APCHO runs parameter optimization based on the UE velocity and HPI control. First, our proposal adjusts the offset value of the execution condition based on the UE's velocity. We adjust only the offset parameter of the execution condition introduced in Equation 3. Initially, APCHO calculates the $o_{\rm exec}$ parameter using Equation 8

for every target cell identified in the measurement report. This step ensures that each target cell's execution condition is tailored to its specific characteristics, paving the way for efficient handover decisions.

$$o_{exec} = log_{hysteresis} \frac{(V_{max} - V_{current} + 1)}{V_{max}}$$
 (8)

where $V_{max'}$ $V_{current}$ are the UE's maximum and current velocities, respectively. Hysteresis is a predefined value, the same as in traditional handover. For example, if the UE's velocity is high, the value of o_{exec} is low. After calculating $o_{exec'}$ the serving cell sends configuration to the UE for monitoring the target cell using Equation 3.

The second step involves incorporating HPI into our calculation. While HPI encompasses three indicators, one stands out when handover errors occur, carrying more weight than the others. Our calculation detects this pivotal indicator and dynamically adjusts the offset to mitigate its impact. This means that the value of $o_{\it exec}$ is finetuned based on the primary indicator's effect on HPI, either increasing or decreasing it as needed. Through this adaptive approach, the algorithm effectively mitigates the overall impact of HPI on system performance. Equation 9 shows these HPI-driven adjustments.

$$o_{exec} = o_{exec} \pm \delta \tag{9}$$

where δ is the predefined adjustment value, and $o_{\rm exec}$ is the current value of $o_{\rm exec}$. For example, when HPP is greater than RLF, APCHO decreases the offset value by δ , but it increases the offset when RLF is greater than HPP.

The third step is to adjust the cell outage threshold based on the difference in cell sizes between the serving and target cells. Equation 10 shows the calculation of $o_{threshold}$. When a UE moves from a macrocell to a microcell, APCHO sets a lower value for $o_{threshold}$. As a result, the UE keep a connection with the macrocell. Conversely, the approach increases the $o_{threshold}$ value as the UE moves away from the microcell.

$$o_{threshold} = o_{threshold} - \frac{s_{serving}}{s_{target}}$$
 (10)

where $S_{serving}$, S_{target} are the size of the serving and target cells, respectively. $o_{threshold}$ is the current threshold.

When the serving cell's signal strength falls below the threshold, APCHO proactively selects the best target cell, preventing delayed handovers and signal drops. On the other hand, when the cell outage condition is satisfied, APCHO initiates the handover, ensuring a seamless transition and minimizing signal loss (Equation 11).

$$RSRP_{serving} \le o_{threshold}$$
 (11)

where $o_{threshold}$ is the cell outage threshold calculated by Equation 10. $RSRP_{serving}$ is the RSRP of the serving cell.

3.2. APCHO PROCEDURES

We implemented a network function in the core network that collects handover information from all cells

and computes the HPI for each pair after every handover procedure. APCHO enables continuous monitoring and uses HPI calculation through the following three steps:

- HPI is calculated using parameter values for each cell combination. If the HPI is higher than the threshold, the necessary parameters need to be adjusted using Equation 9,
- The impact of the three HPI indicators is assessed and prioritized based on their influence. The parameter with the greatest impact is identified, and its associated function is used to fine-tune its value accordingly,
- 3. The HPI is then recalculated.

The message flows of APCHO are presented in Fig. 2.

If the add condition is satisfied (Equation 1), candidate cells are added to the target cell list. The serving cell determines the appropriate values for the offset of the execution condition using Equation 3 and the cell outage threshold using Equation 10.

- **Step 1** Measurement command and report: The preparation phase begins when the serving cell sends a measurement command. The UE replies to the serving cell with a report.
- **Step 2** CHO decision and add condition: on receiving the report, the serving cell makes the CHO decision based on Equation 1.
- **Step 3** HO request: if a handover is necessary, the serving cell sends handover requests to all candidate cells that have just been added to target cell list.

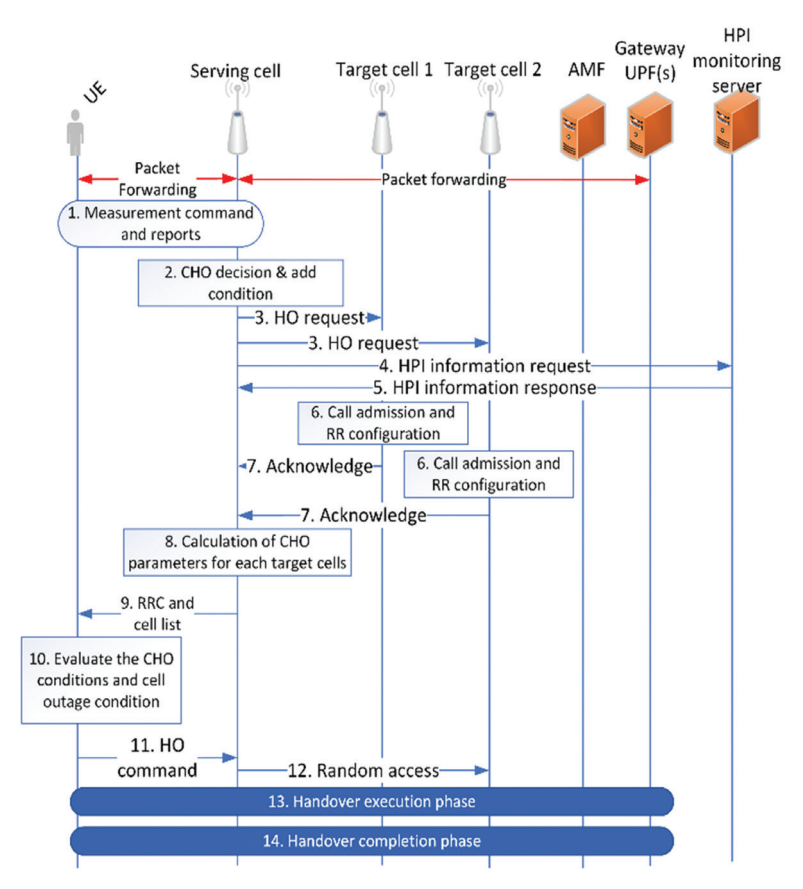


Fig. 2. The message flows of APCHO

- **Step 4** HPI information request: simultaneously, the serving cell sends an HPI information request to the calculation server.
- **Step 5** HPI information response: the calculation server responds with HPI information for each combination of the serving and target cells. The calculation server already calculated HPI information based on the handover historical information.
- **Step 6** Call admission and RR configuration: the target cells accept the handover request and prepare radio resources (RR) for the UE's active services.
- **Step 7** Acknowledge: the target cells send an acknowledgment to the serving cell. This acknowledgment includes all information needed for the next phases of the handover procedure.
- **Step 8** Calculation of CHO parameters for each target cells: After receiving all acknowledgments and necessary information, the serving cell calculates the execution parameter $o_{\it exec}$ based on Equation 8 and 9, and the cell outage parameter $o_{\it threshold}$ based on Equation 10 for each target cell.
- **Step 9** RRC and cell list: the serving cell sends a configuration message that includes RRC configuration,

target cell list, and parameters of the execution and cell outage conditions.

Step 10 – Evaluate the CHO conditions and cell outage condition: the UE monitors the target cell list using the CHO conditions and cell outage condition.

Step 11 – HO command: if one of conditions is met, the UE notifies the serving cell and begins the handover execution phase with the selected target cell.

The algorithm starts by initializing the test environment. When the user approaches the edge of the serving cell, the UE sends a measurement report. The serving cell checks neighboring cells against predefined add conditions, creates a target cell list, and decides whether to initiate a handover. If needed, it sends handover requests to the target cells and simultaneously requests additional data from the Handover Performance Indicator (HPI) control server.

After receiving the responses, the serving cell calculates execution and cell outage condition parameters for each target and sends them to the UE. The UE continuously monitors these target cells and initiates handover execution if either the execution condition or the cell outage condition is satisfied. If neither condition is met, the algorithm loops back to reevaluate conditions in the next cycle. Fig. 3 illustrates this iterative process with a blue dashed line labelled "Evaluate CHO and cell outage conditions."

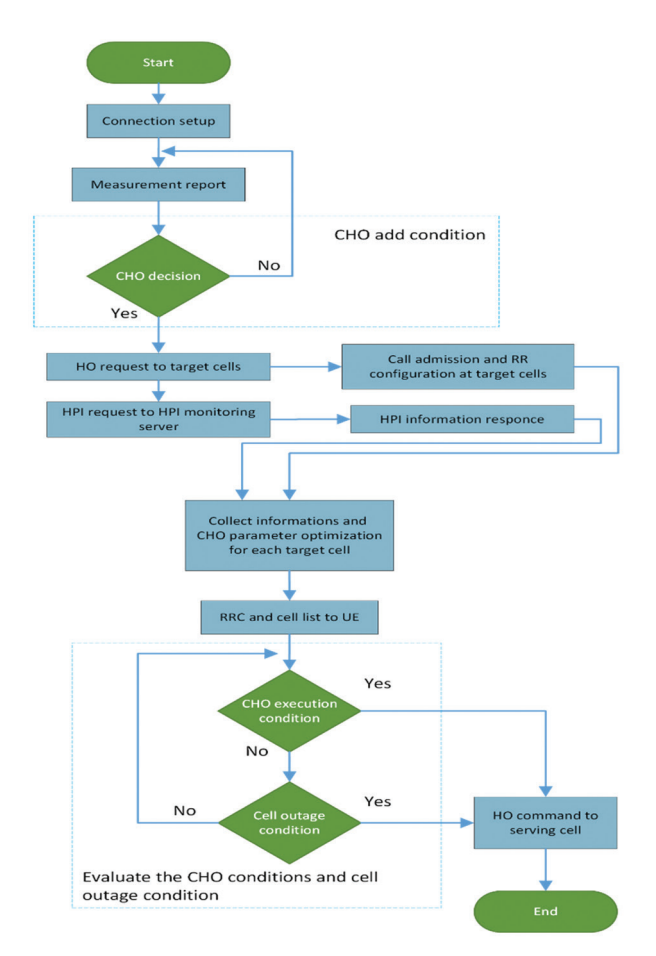


Fig. 3. The flowchart of APCHO

We excluded the CHO remove condition from this flow and focused instead on evaluating the CHO decision logic and performance.

4. SIMULATION RESULTS

In this section, we compare APCHO in a simulation against a standard CHO, a velocity and cell outage-based version. The evaluation is based on handover errors and RLF, averaged over 50 simulation runs using the topology shown in Fig. 4. We started with 100 users and increased the number of users by 100 for each of the 50 runs. The velocity was randomly assigned when placing users at the beginning of the simulation. Additionally, we ensured that 50% of the users had a velocity of less than 80 km/h. Table 1 outlines the parameters used in the simulation. The network topology was implemented with macrocells and microcells added at random locations. The topology advantage of 5G and beyond networks is the microcell and its performance. In [29], the authors introduced the usage of microcell's mode, power consumption, and a heterogeneous dense network topology.

Fig. 5 shows the average RLF ratio, defined as the ratio between the number of RLFs and the number of users. The graph illustrates that RLF ratio for the standard CHO and cell outage mechanism is 2%-6% higher than that of APCHO as the number of handover attempts increases. This is because the static parameters of CHO and cell-outage condition have low effectiveness in preventing too late handovers.

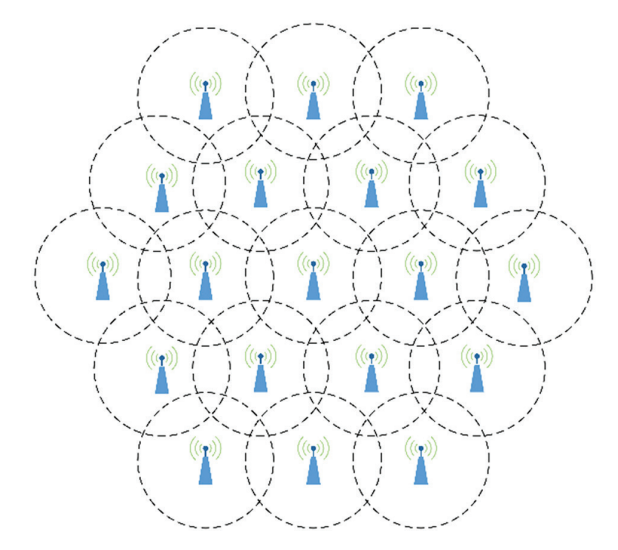


Fig. 4. The simulation topology with 19 macrocell

Note that the number of users and number of attempted handovers are directly related. The velocity-based mechanism produces an RLF ratio is 1%-3% higher than APCHO because $o_{\it exec}$ is adjusted based on only on velocity. As a result, at 1000 users, the RLF ratio in APCHO is 2%,5%, 6% lower than in the other three mechanisms. This is because APCHO optimizes the parameters using three mechanisms: execution condition parameters, cell outage condition, and HPI calculation-based changes.

Table 1. Simulation parameters

Parameters	Macrocell	Microcell	
Carrier frequency (GHz)	2.1	2.1	
Bandwidth (MHz)	20	100	
The numbers of cells	19	30	
Cell radius (m)	500	200	
Path loss model	128.1+37.6 log10 (d)	128.1+37.6 log10 (d)	
Transmit Power (dBm)	43	21	
Overlapping zone (%)	30	0	
Antenna Gain (dBi)	5	5	
Antenna Gain of UE (dBi)	0	0	
Shadowing (dB)	12	7.8	
The number of UEs	Up to 1000 (each simulation runs 100 to 1000)		
Velocity of UEs, V_{max} (km/h)	Up to 200 (each user randomly selected)		
UE's mobility model	Random direction		
HPI threshold (%)	2		
o _{add} , o _{remove} , o _{threshold} (dB)	9 dB, 6 dB, -8 dB		
$\omega_{{\scriptscriptstyle HPP'}}$, $\omega_{{\scriptscriptstyle RLF'}}$, $\omega_{{\scriptscriptstyle HOF}}$	1,1,1		

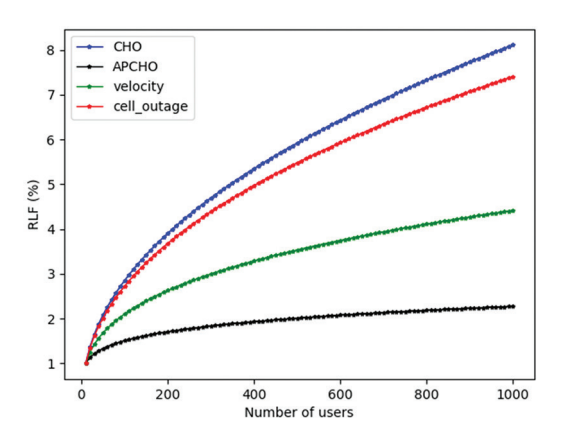


Fig. 5. RLFs versus Number of users

Fig. 6 shows the results for RLFs at velocities ranging from 10 km/h to 200 km/h for all four mechanisms. Below 40 km/h, all four mechanisms show low differences between standard CHO, the velocity-based mechanism, the cell outage-based mechanism and APCHO. The cell-outage mechanism and standard CHO showed similar results at low velocities. On the contrary, it reduced the number of handovers from macrocell to microcell. Starting from 50 km/h, our APCHO and the velocity-based mechanism show a lower growth rate in RLFs compared to the other two mechanisms. The proposed APCHO maintains low RLFs at all velocities, even at 200 km/h.

This effect is achieved through the dynamic adjustment of $o_{\rm exec}$ and $o_{\rm threshold}$. However, as velocity increases beyond 150 km/h, RLFs begin to increase due to the lower RSRP of the serving cell and delayed handovers. CHO and cell-outage mechanisms show a higher growth rate in RLFs. This is because, in these mechanisms, the cell-outage condition is only one of the factors influencing handover decisions, which allows the UE to begin a handover with the target cell too late. We show the average percentage of handover errors with respect to the number of users and their velocity.

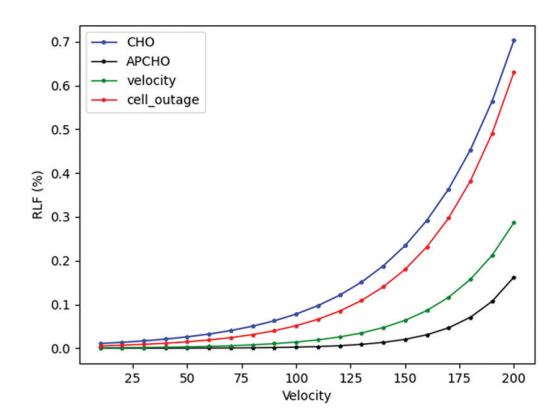


Fig. 6. RLFs versus velocity

Handover errors refer to the number of procedure failures that occur when the UE's handover procedure fails during the execution or completion phases.

Fig. 7 illustrates the comparison of handover errors across four combinations of UE numbers and velocity: low UE density with low velocity (low-low), low UE density with high velocity (low-high), high UE density with low velocity (high-low), and high UE density with high velocity (high-high) environments. Low UE density refers to 100-250 users, while high density refers to up to 1000 users in the simulation area.

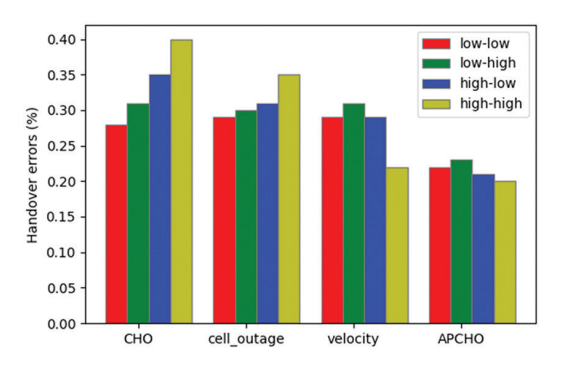


Fig. 7. Handover errors versus the four combinations of UE and velocity

Similarly, low velocity means 10-80 kmph and high velocity means 80-200 kmph. As observed in Figure 6, the baseline CHO shows handover errors of approximately 0.4% in the high-high environment. This is due to the higher number of users, which results in more ping-pong handovers, handover failures, too early handovers, and too late handovers. Additionally, as UE density increases, more handover procedures are attempted, which affects the percentage of handover errors. The velocity-based and APCHO show reduced handover errors in high-low and high-high combinations. The proposed APCHO has few handover errors at all combinations. This is because the server calculates HPI based on handover historical data, and APCHO adjusts the handover parameters for each handover and combinations of target and serving cell.

Fig. 8 illustrates handover performance over the 40-minute test duration. At the start of the simulation

(before 4 minutes), there were minimal differences between APCHO and the velocity-based mechanisms.

As handover failures and the impact of moving velocity began to emerge, the handover error for CHO and cell outage-based mechanism increased noticeably. Notably, CHO displayed a peak and continuous increase, reaching 12% handover errors at 40 minutes. In contrast, the proposed APCHO improved performance by adjusting $o_{\it exec}$ for each attempted handover. This led to a reduced HPI compared to CHO, especially after 5 minutes into the simulation.

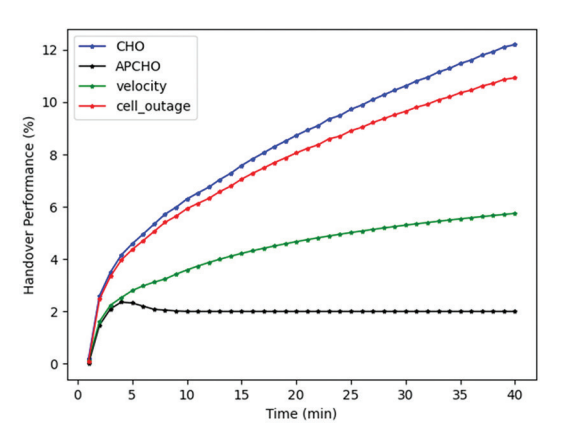


Fig. 8. Performance comparison of mechanisms

As shown in Table 2, the proposed APCHO reduces RLF, ping-pong handovers, and overall handover errors. For example, when $\omega_{\rm HPP}$ and $\omega_{\rm HOF}$ are set to 1 and $\omega_{\rm RLF}$ is changed from 1 to 10, RLF decreased by 2.142%, while HPP and HOF increased by 2.147% and 0.08%, respectively. When adjusting the weighting factors, HOF variation is smaller compared to the variation in HPP and RLFs. For example, when $\omega_{\rm RLF}$ and $\omega_{\rm HPP}$ are set to 1 and $\omega_{\rm HOF}$ is increased from 0.1 to 10, HOF changes by only 0.4%. Therefore, by adjusting the weights of the reward function, the RLFs and HPP experienced by users can be reduced through the optimization of specific types of HO errors.

Table 2. Effect of weight parameters

Weights	Too-early and ping-pong handovers	Too late handovers or RLF	Handover errors
ω_{HPP} =1, ω_{RLF} =1, ω_{HOF} =1	5.364	4.385	1.158
ω_{HPP} =1, ω_{RLF} =10, ω_{HOF} =1	7.511	2.243	1.156
ω_{HPP} =10, ω_{RLF} =1, ω_{HOF} =1	3.318	4.391	1.206
$\omega_{{\scriptscriptstyle HPP}}$ =1, $\omega_{{\scriptscriptstyle RLF}}$ =10, $\omega_{{\scriptscriptstyle HOF}}$ =0.1	5.465	2.158	1.201
ω_{HPP} =10, ω_{RLF} =1, ω_{HOF} =0.1	3.248	4.355	1.92
ω_{HPP} =1, ω_{RLF} =1, ω_{HOF} =10	5.344	3.401	1.116

5. CONCLUSION

We have introduced Autotuning-based Parameters for Conditional Handover (APCHO), an enhanced version of CHO that incorporates autotuning parameters and second handover trigger to improve 5G handover performance. In addition, we calculated the HPI to au-

tomatically adjust parameters when error thresholds were exceeded. Our proposed APCHO mechanism also uses mobility management performance data to dynamically adjust the weight of parameters to mitigate handover errors impact. We evaluated the mobility performance using a simulator for 5G HetNets. The simulation results showed that APCHO reduced HOF and RLFs compared to standard CHO.

ACKNOWLEDGEMENTS

This work was supported by the National University of Mongolia, grant number P2022-4381.

6. REFERENCES:

- [1] U. Gustavsson, P. Frenger, C. Fager, T. Eriksson, H. Zirath, F. Dielacher, C. Studer, A. Pärssinen, R. Correia, J. N. Matos, D. Delo, N. B. Carvalho, "Implementation challenges and opportunities in beyond-5G and 6G communication", IEEE Journal of Microwaves, Vol. 1, No. 1, 2021, pp. 86-100.
- [2] I. M. Abbas, T. Y. Hoe, C. Ali, A. D. Jamal, "Handover Optimization Framework for Next-Generation Wireless Networks: 5G, 5G— Advanced and 6G", Proceedings of the IEEE International Conference on Automatic Control and Intelligent Systems, Shah Alam, Malaysia, 29 June 2024, pp. 409-414.
- [3] I. Begić, A. S. Kurdija, Željko Ilić, "A Framework for 5G Network Slicing Optimization using 2-Edge-Connected Subgraphs for Path Protection", International Journal of Electrical and Computer Engineering Systems, Vol. 15, No. 8, 2024, pp. 675-685.
- [4] D. Chandramouli, R. Liebhart, J. Pirskanen, "5G for the Connected World", 1st Edition, John Wiley & Sons, 2019.
- [5] H. Martikainen, I. Viering, A. Lobinger, T. Jokela, "On the basics of conditional handover for 5G mobility", Proceedings of the IEEE 29th Annual International Symposium on Personal, Indoor and Mobile Radio Communications, Bologna, Italy, 9-12 September 2018, pp. 1-7.
- [6] I. Viering, H. Martikainen, A. Lobinger, B. Wegmann, "Zero-zero mobility: Intra-frequency handovers with zero interruption and zero failures", IEEE Network, Vol. 32, No. 2, 2018, pp. 48-54.
- [7] Intel, "3gpp tdocs, performance evaluation of conditional handover", Intel Corporation, Chengdu, China, Technical Report R2-1814052, No. R2-103b, 2018.
- [8] Nokia, "3gpp, conditional handover basic aspects and feasibility in rel-15", Nokia Shanghai Bell, Berlin, Technical Report R2-1708586, No. R2-99, 2017.
- [9] U. Karabulut, A. Awada, I. Viering, A. N. Barreto, G. P. Fettweis, "Analysis and performance evaluation of con-

- ditional handover in 5G beamformed systems", arX-iv:1910.11890, 2019.
- [10] J. Stanczak, U. Karabulut, A. Awada, "Conditional handover in 5G-principles, future use cases and FR2 performance", Proceedings of the International Wireless Communications and Mobile Computing, Dubrovnik, Croatia, 30 May 3 June 2022, pp. 660-665.
- [11] W. K. Saad, I. Shayea, B. J. Hamza, H. Mohamad, Y. I. Daradkeh, W. A. Jabbar, "Handover parameters optimisation techniques in 5G networks", Sensors, Vol 21, No. 15, 2021, pp. 1-22.
- [12] S. B. Iqbal, A. Awada, U. Karabulut, I. Viering, P. Schulz, G. P. Fettweis, "On the modeling and analysis of fast conditional handover for 5g-advanced", Proceedings of the IEEE 33rd Annual International Symposium on Personal, Indoor and Mobile Radio Communications, Kyoto, Japan, 12-15 September 2022, pp. 595-601.
- [13] S. B. Iqbal, S. Nadaf, A. Awada, U. Karabulut, P. Schulz, G. P. Fettweis, "On the analysis and optimization of fast conditional handover with hand blockage for mobility", IEEE Access, Vol. 11, 2023, pp. 30040-30056.
- [14] C. Fiandrino, D. J. Martínez-Villanueva, J. Widmer, "A study on 5G performance and fast conditional handover for public transit systems", Computer Communications, Vol. 209, 2023, pp. 499-512.
- [15] J. Stanczak, U. Karabulut, A. Awada, "Conditional handover modelling for increased contention free resource use in 5g-advanced", Proceedings of the IEEE 34th Annual International Symposium on Personal, Indoor and Mobile Radio Communications, Toronto, ON, Canada, 5-8 September 2023, pp. 1-6.
- [16] E. Kim, I. Joe, "Handover triggering prediction with the two-step xgboost ensemble algorithm for conditional handover in non-terrestrial networks", Electronics, Vol. 12, No. 16, 2023, pp. 1-24.
- [17] A. Gharouni, U. Karabulut, A. Enqvist, P. Rost, A. Maeder, H. Schotten, "Signal overhead reduction for Al-assisted conditional handover preparation", Proceedings of Mobile Communication-Technologies and Applications; 25th ITG-Symposium, Osnabrueck, Germany, 3-4 November 2021, pp. 1-6.
- [18] A. Alhammadi, M. Roslee, M. Y. Alias, I. Shayea, S. Alraih, K. S. Mohamed, "Auto tuning self-optimization algorithm for mobility management in LTE-A and 5G Het-Nets", IEEE Access, Vol. 8, 2019, pp. 294-304.
- [19] S. Deb, M. Rathod, R. Balamurugan, S. K. Ghosh, R. K. Singh, S. Sanyal, "Performance evaluation of conditional handover in 5G systems under fading scenario", arXiv:2403.04379, 2024.

- [20] S. Deb, M. Rathod, R. Balamurugan, S. K. Ghosh, R. K. Singh, S. Sanyal, "Evaluating Conditional handover for 5G networks with dynamic obstacles", Computer Communications, Vol. 233, 2025, p. 108067.
- [21] C. F. Kwong, S. Chenhao, L. Qianyu, Y. Sen, C. David, K. Pushpendu, "Autonomous handover parameter optimisation for 5G cellular networks using deep deterministic policy gradient", Expert Systems with Applications, Vol. 246, 2024, pp. 1-8.
- [22] C. Lee, H. Cho, S. Song, J. M. Chung, "Prediction-based conditional handover for 5G mm-wave networks: A deep-learning approach", IEEE Vehicular Technology Magazine, Vol. 15, No. 1, 2020, pp. 54-62.
- [23] T. Y. Arif, A. Fitri, "Adaptive Strategies and Handover Optimization in 5G Networks to Address High Mobility Challenges", Proceedings of the IEEE International Conference on Electrical Engineering and Informatics, Banda Aceh, Indonesia, 12-13 September 2024, pp. 153-157.
- [24] Z. Yin, "Mobility Performance Analysis for Mixed Handover", Proceedings of the IEEE Wireless Communications and Networking Conference, Dubai, United Arab Emirates, 21-24 April 2024, pp. 1-6.
- [25] S. C. Sundararaju, R. Shrinath, P. B. Dandra, P. Vanama, "Advanced Conditional Handover in 5G and Beyond Using Q-Learning", Proceedings of the IEEE Wireless Communications and Networking Conference, Dubai, United Arab Emirates, 21-24 April 2024, pp. 1-6.
- [26] Y. S. Junejo, K. S. Faisal, S. C. Bhawani, E. Waleed, "Adaptive Handover Management in High-Mobility Networks for Smart Cities", Computers, Vol. 14, No. 1, 2025, pp. 1-27.
- [27] S. O. Hasan, S. K. Ezzulddin, O. S. Hammd, R. H. Mahmud, "Design and Performance Analysis of Rectangular Microstrip Patch Antennas Using Different Feeding Techniques for 5G Applications", International Journal of Electrical and Computer Engineering Systems, Vol. 14, No. 8, 2023, pp. 833-841.
- [28] I. M. Abbas, T. Y. Hoe, C. Ali, A. D. Jamal, "Self-optimization of handover control parameters for 5G wireless networks and beyond", IEEE Access, Vol. 12, 2023, pp. 6117-6135.
- [29] J. Premalatha, A. S. A. Nisha, S. E. V. Somanathan Pillai, A. Bhuvanesh, "Performance Measurement of Small Cell Power Management Mechanism in 5G Cellular Networks using Firefly Algorithm", International Journal of Electrical and Computer Engineering Systems, Vol. 15, No. 5, 2024, pp. 437-448.